Bimalesh Giri
Banabir Pal
Prajwal Rigvedi
Abhay Srivastava
Katayoon Mohseni
Anupam Singh
Arthur Ernst (JKU Linz)
A. Ney (JKU Linz)
J.M. Tonnerre (CNRS Gr.)

Stuart S.P. Parkin

Synchrotron X-Ray Analysis of Magnetic Nanosystems

- Holger L. Meyerheim (MPI f. Mikrostrukturphysik)

http://www.mpi-halle.mpg.de

Magnetic Data Storage: hard disk drives to racetrack memory and Skyrmions

- Data is stored within the boundaries between oppositely magnetized regions (up/down and down/up)

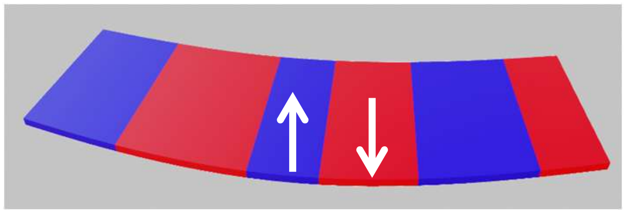

1956

First hard drive
IBM 350 disk storage unit
5 MB capacity (0.0001 GB/inch^2)

2021

SEAGATE HAMR device
20 TB capacity (2,000 GB/inch^2)

- ~50 year old technology
- Mechanical device
- 2D design
- Size cannot be reduced further because of thermal fluctuations

Racetrack Memory

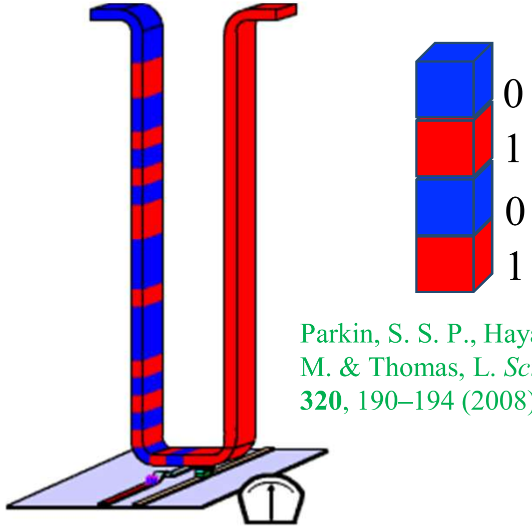

Parkin, S. S. P., Hayashi, M. & Thomas, L. *Science* **320**, 190–194 (2008)

- Data stored in domain walls
- No mechanical parts
- 3D design

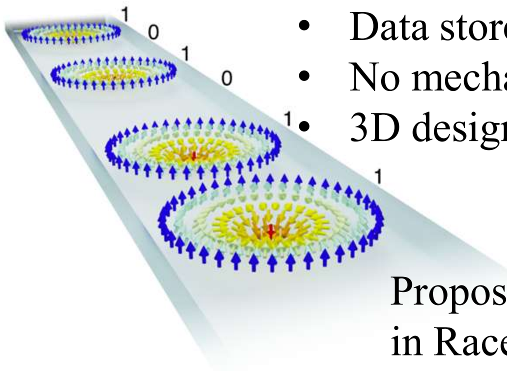

Proposed: Skyrmions in Racetrack

Dzyaloshinskii-Moriya Interaction (DMI) and Skyrmions

- DMI arises in acentric magnetic crystals
- Stabilizes spin canting >> Skyrmions

H =

$- \sum_{\langle i,j \rangle} J_{ij} (S_i \cdot S_j)$ [Heisenberg]

$- \sum_{\langle i,j \rangle} D_{ij} \cdot (S_i \times S_j)$ [DMI]

$+ (\mu_0/4\pi) \sum_{\{i<j\}} [(m_i \cdot m_j - 3 (m_i \cdot \hat{r}_{ij})(m_j \cdot \hat{r}_{ij})) / r_{ij}^3]$ [Dipol]

$- K \sum_i (S^z_i)^2$ [Anisotropy]

$- \mu \sum_i (B \cdot S_i)$ [Zeeman]

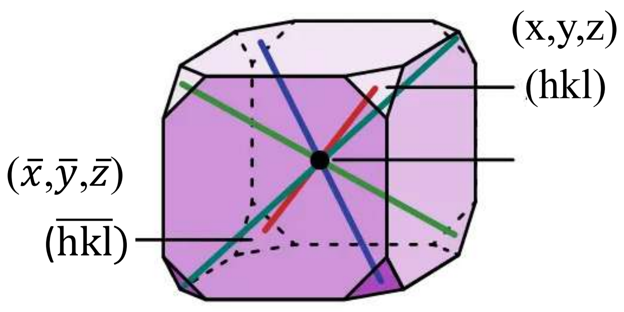

centrosymmetric

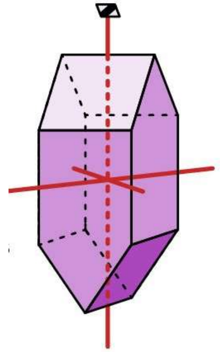

acentric

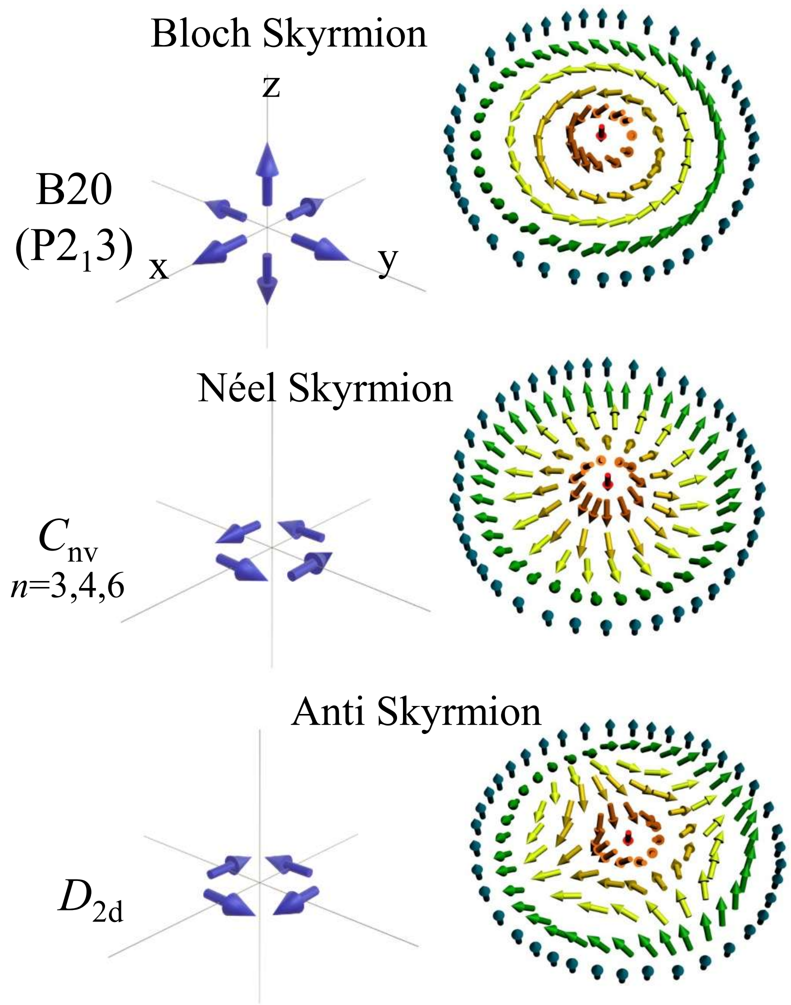

Observation of Skyrmions by Lorentz Transmission Microscopy

Electron beam

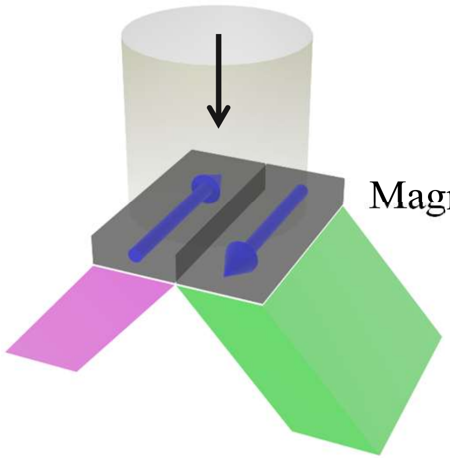

Magnetic sample

Transmitted beam
Increased intensity (white)
Decreased intensity (black)

$$\boldsymbol{F} = -e(\boldsymbol{v} \times \boldsymbol{B})$$

LTEM contrast is sensitive only to the in-plane components of magnetization
→ ~5 nm spatial resolution
→ >~5 nm thick material can be detected

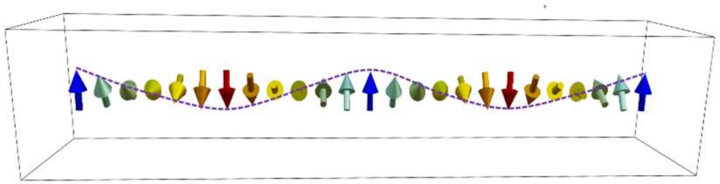

Spin helix

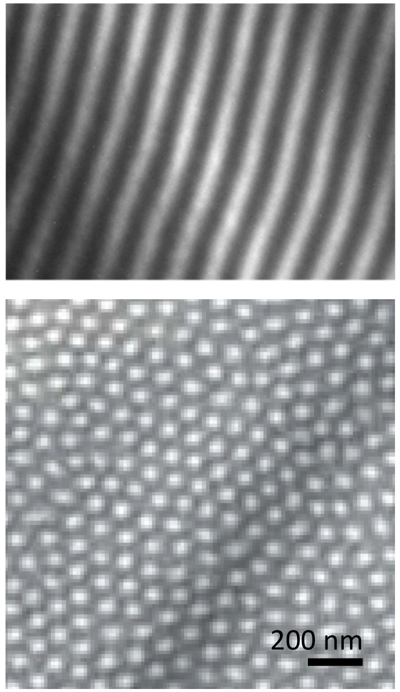

First real-space observation of Bloch skyrmions in $Fe_{0.5}Co_{0.5}Si$ using LTEM

Yu, X., Onose, Y., Kanazawa, N. *et al.* *Nature* **465,** 901–904 (2010).

Crystal structure of $LaMn_2Ge_2$ and Neèl Skyrmions

Space group I4/mmm (139) ⟷ ??

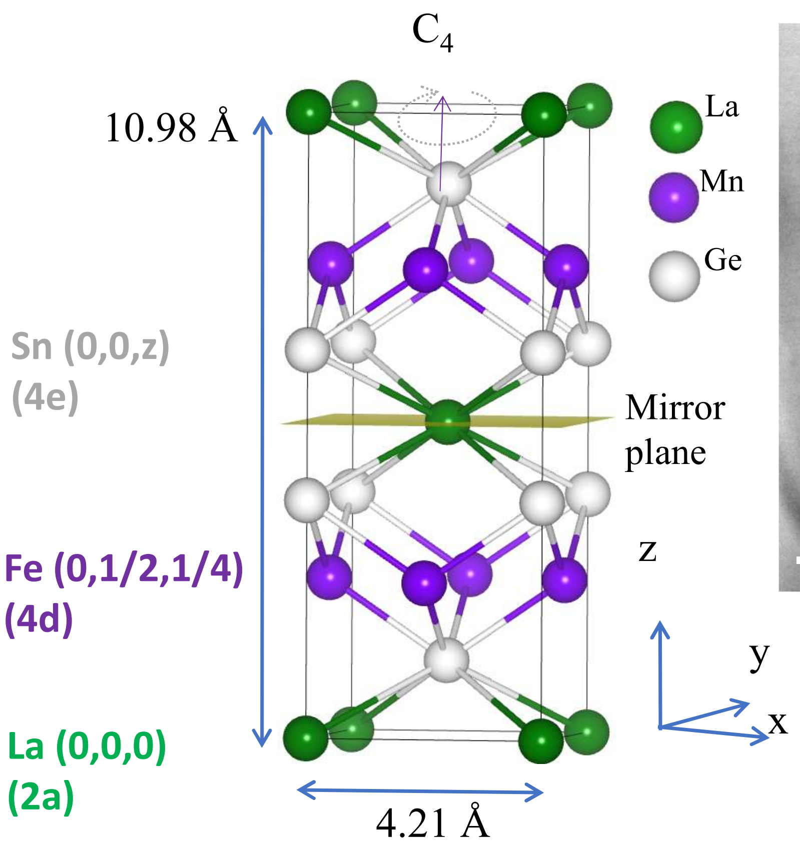

Néel Skyrmions LTEM

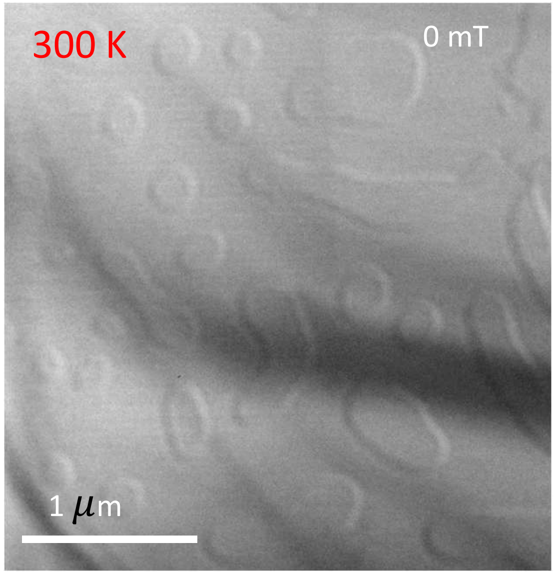

Néel Skyrmions Simulation

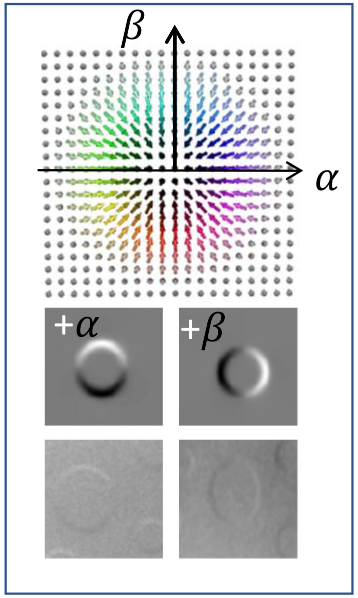

Topological Charge Q=-1

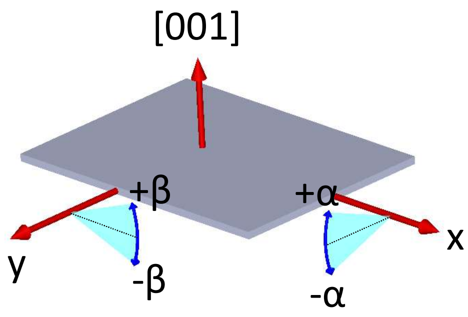

Asymmetric contrast when the sample is tilt

Experiment at Petra III (beamline P24)

M. Tolkiehn,
L. Noohinejad

Four Circle Euler Geometry (E_0=24 keV)

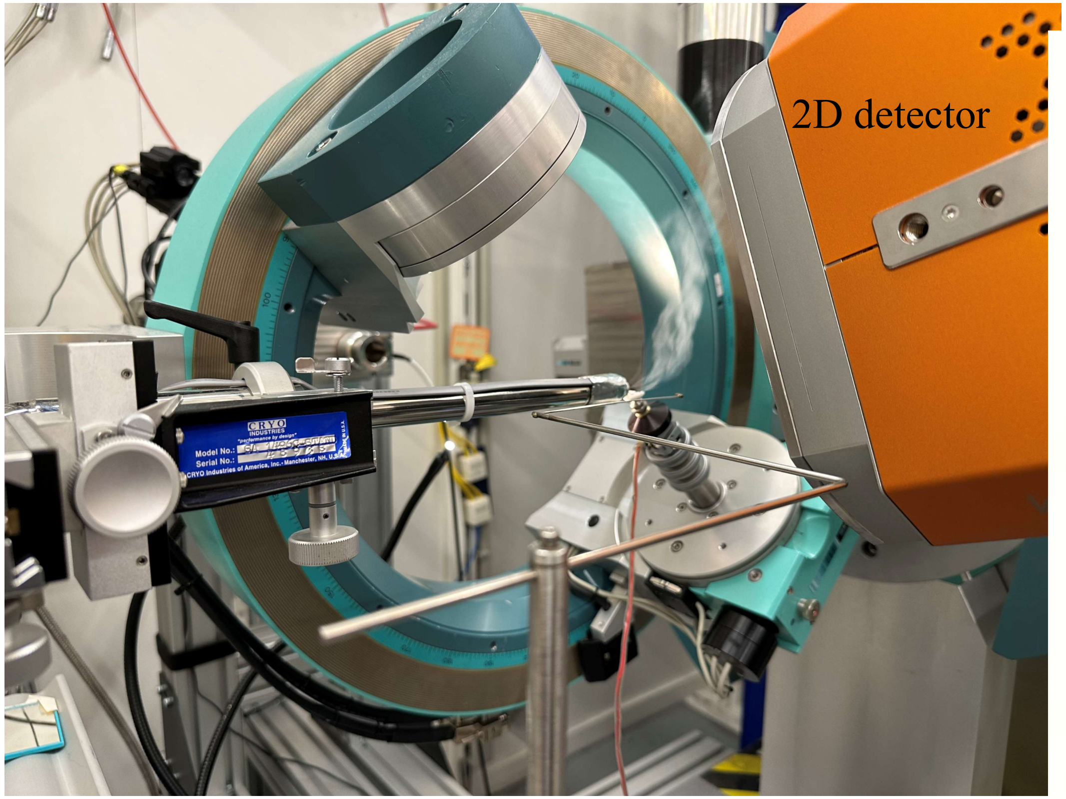

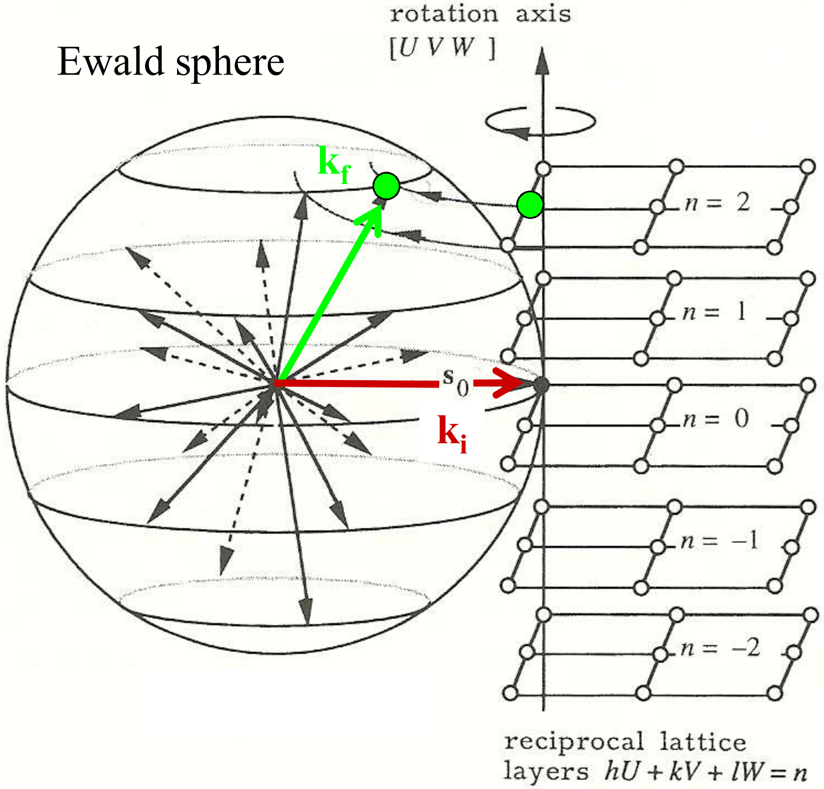

X-ray diffraction in detail: Measurement of integrated intensities

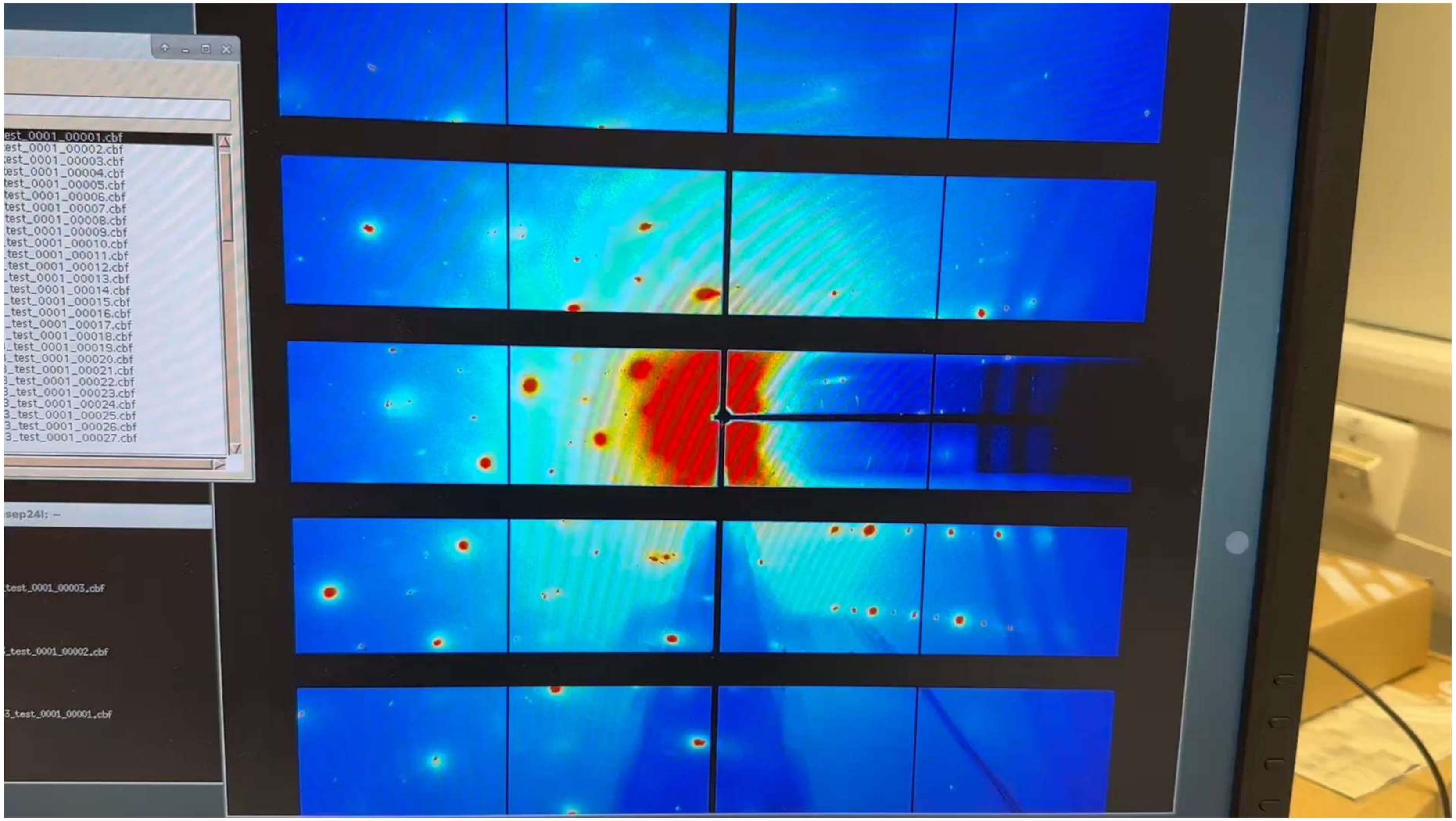

Measurement of
2000-10000
reflections
in 360 sec.

X-ray diffraction in detail: Structural refinement

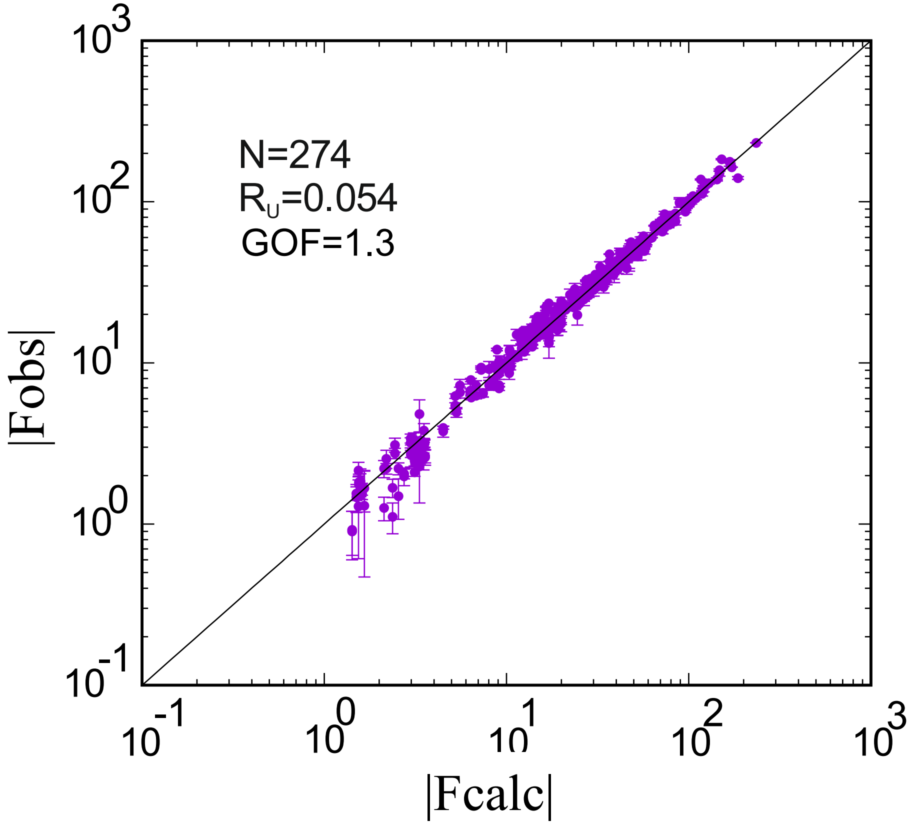

Fit quality parameters:

$$R_u = \frac{\sum_{hkl} \big| |F_{obs}| - |F_{calc}| \big|}{\sum_{hkl} |F_{obs}|}$$

$$GOF = \sqrt{\frac{1}{N-P} \sum_{hkl} (|F_{obs} - F_{calc}|)^2 / \sigma^2}$$

Structural refinement with Debye –Waller factor in harmonic approximation

- $$F(\vec{q}) \propto \sum_{\alpha} f_{\alpha} \exp(-2\pi i \vec{q}\cdot\vec{r_{\alpha}}) \cdot T_{\alpha}^{\mathrm{H}}(\vec{q})$$

$$T_{\alpha}^{\mathrm{H}}(\vec{q}) = \exp\left(-8\pi^2 U_{\alpha}^{kl} q_k q_l\right)$$

$$\begin{pmatrix} U11 & U12 & U13 \\ U21 & U22 & U23 \\ U31 & U32 & U33 \end{pmatrix}$$

Debye Waller Factor (Gaussian)

Corresponding real space representation:
Probability density function (PDF)

$$\mathrm{PDF}^{\mathrm{H}}(\vec{u}) = \sqrt{\frac{\det(U_{\alpha}^{-1})}{(2\pi)^3}} \exp\left(-\frac{1}{2}\vec{u}^T U_{\alpha}^{-1}\vec{u}\right)$$

$$\vec{u} = \vec{r} - \vec{r_{\alpha}}$$

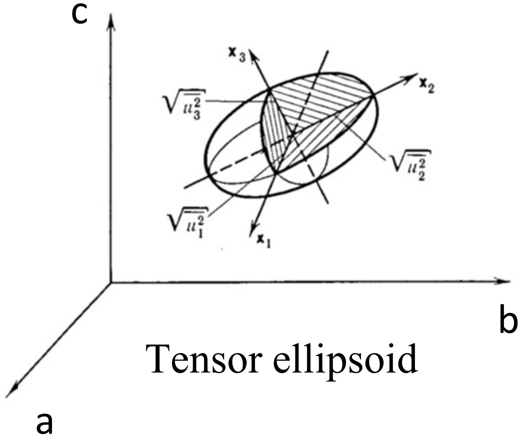

Tensor ellipsoid

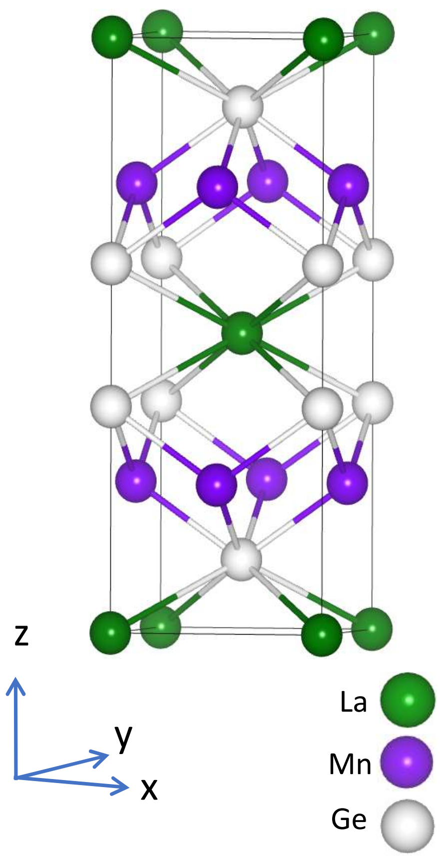

Generalization of Debye –Waller Factor including anharmonic contributions:

$$F(\vec{q}) \propto \sum_{\alpha} f_{\alpha} \exp\left(-2\pi i \vec{q} \cdot \vec{r_{\alpha}}\right) \cdot T_{\alpha}^{\mathrm{H}}(\vec{q})$$

$$T_{\alpha}^{\mathrm{GC}}(\vec{q}) = T_{\alpha}^{\mathrm{H}}(\vec{q}) \left[1 + \frac{1}{3!}(2\pi i)^3 \cdot q_k q_l q_m \cdot C_{\alpha}^{klm} \; (10) + \frac{1}{4!}(2\pi i)^4 \cdot q_k q_l q_m q_n \cdot D_{\alpha}^{klmn} \right] \quad (15)$$

In 4mm symmetry only

$C^{113} = C^{223} \neq 0$

$C^{333} \neq 0$

Gram-Charlier-Representation;
F. W. Kuhs, J. Appl. Cryst. Acta Cryst. (1992). **A48**, 80-98

Corresponding real space representation by Fourier Transformation (analytically):
Probability density function (PDF)

$$\mathrm{PDF}^{\mathrm{GC}}(\vec{u}) = \mathrm{PDF}^{\mathrm{H}}(\vec{u}) \left[1 + \frac{1}{3!} C^{klm} H_{klm}(\vec{u}) + \frac{1}{4!} D^{klmn} H_{klmn}(\vec{u}) \right]$$

$$\vec{u} = \vec{r} - \vec{r_{\alpha}}$$

→ deviation from ellipsoidal shape

Structural refinement including anharmonic contributions to thermal disorder

Refinement: R_U versus C^{113} & C^{333}

296K (I4mm)

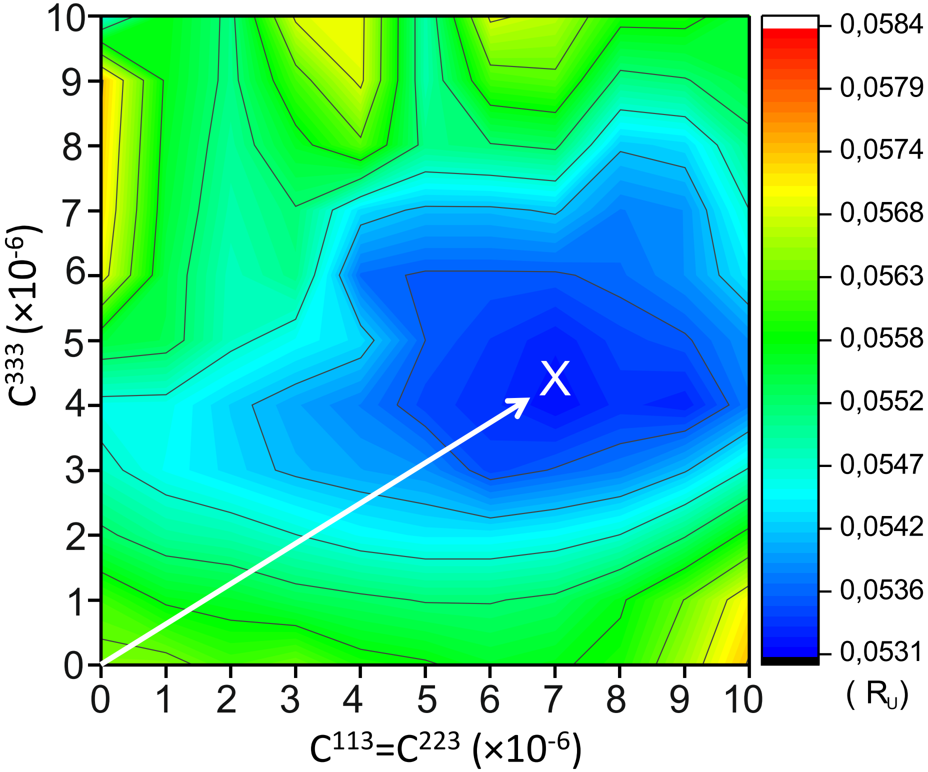

200K (I4/mmm) inversion symmetric

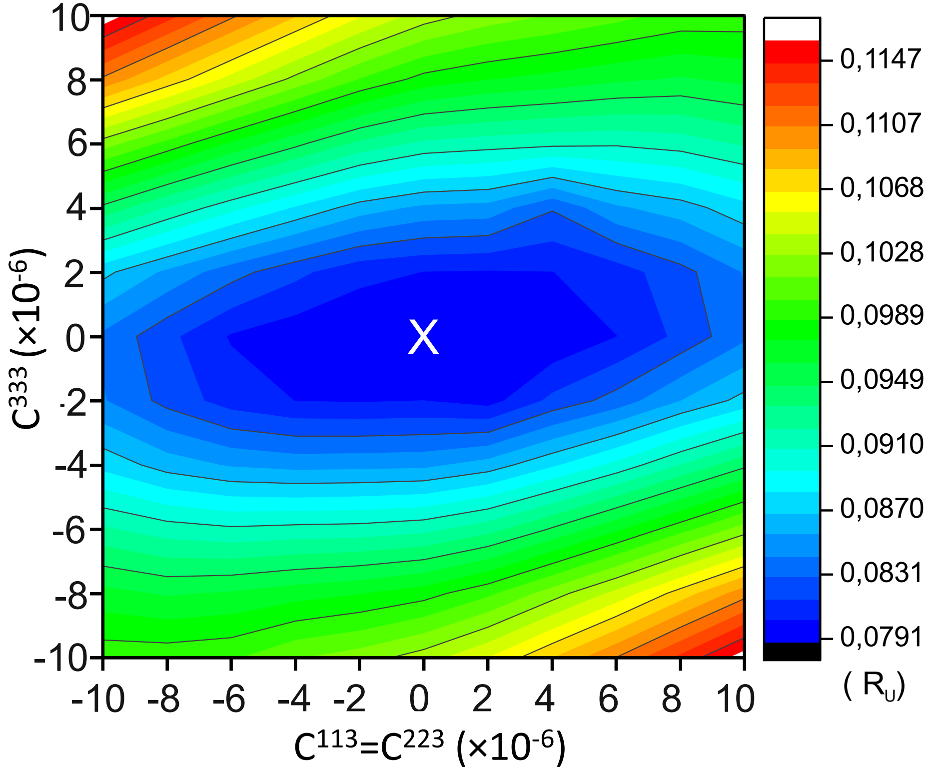

Structural Refinement including anharmonic contributions to thermal disorder

Normalized difference:

$$\Delta PDF = \frac{PDFGC3 - PDFH}{PDFH}$$

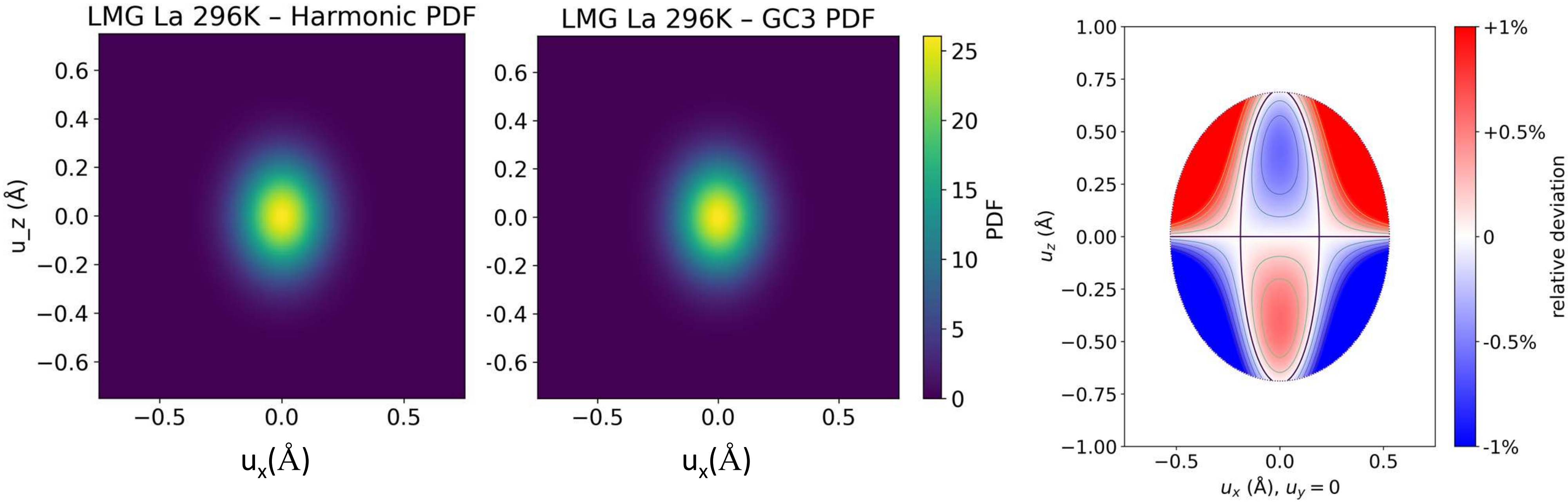

Anharmonic atomic displacement parameters: Cs monosheet

$$T_\alpha^{\mathrm{GC}}(\vec{q}) = T_\alpha^{\mathrm{H}}(\vec{q})\left[1 + \frac{1}{3!}(2\pi i)^3 \cdot q_k q_l q_m \cdot C_\alpha^{klm} + \frac{1}{4!}(2\pi i)^4 \cdot q_k q_l q_m q_n \cdot D_\alpha^{klmn}\right]$$

=0

12 reflections (hk0)
Fit quality:
GOF: 1.4 >> 0.8
R_U: 12.7% >> 8.5%

Cs/Cu(001): 2D structure
cmm2 plane group symmetry
Debye-temperature =38 K

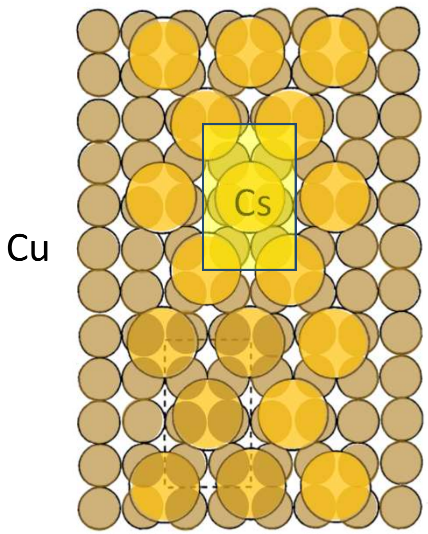

Probability density of Cs atom.

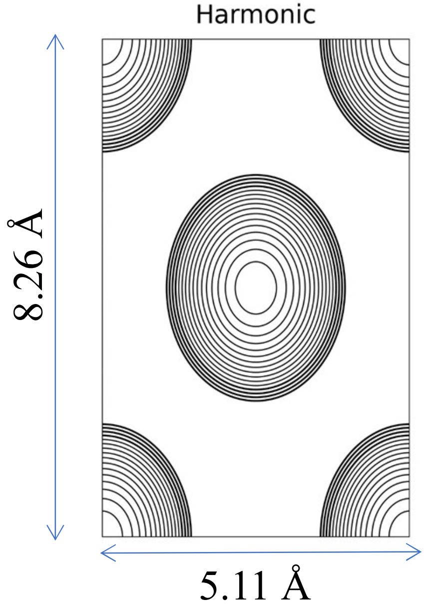

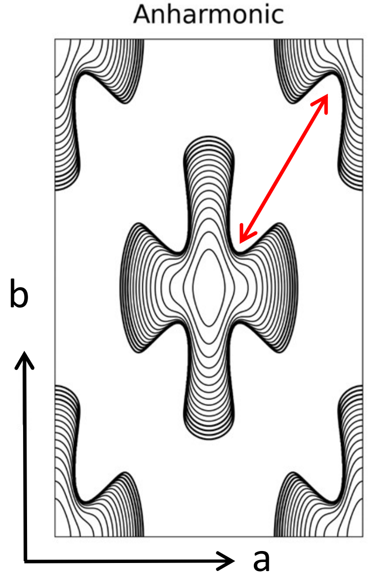

- $U^{11} = 0.10$ Å²
- $U^{22} = 0.16$ Å²
- $D^{1111} = 0.07\times10^{-4}$
- $D^{2222} = 0.22\times10^{-4}$
- **$D^{1122} = -0.11\times10^{-4}$**

Experiments at NSLS (I)
Beamline X16 A (Bell Labs) 1992

Meyerheim, Moritz, Schulz, Eng, Robinson, Surf. Sci. **331-333** (1995) 1422
Habilitation Thesis LMU Munich (1995)

Symmetry breaking in the two-dimensional limit: 1H-$TaSe_2$

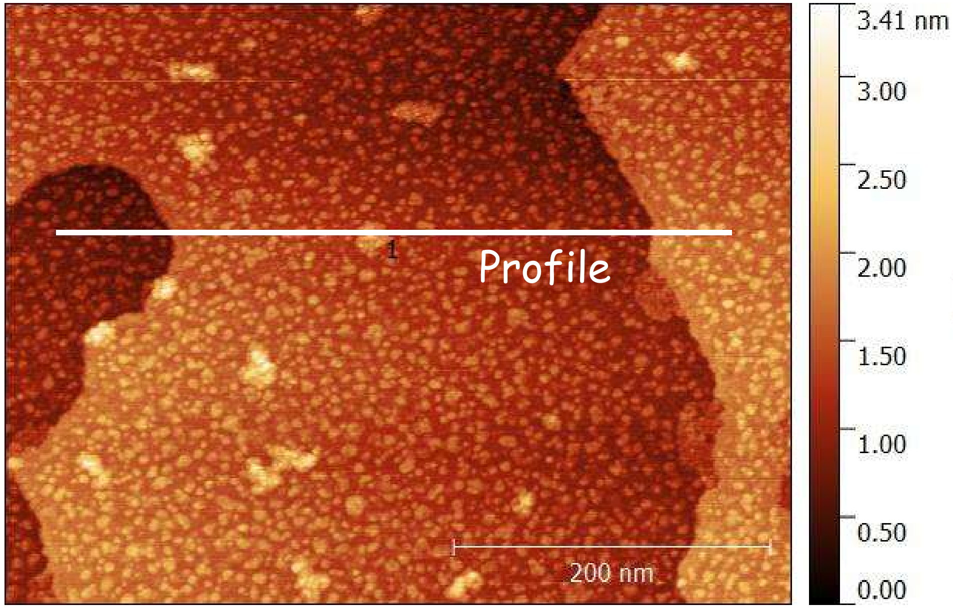

STM: (U= -1 V, I=100 pA)

A. Polyakov, et al. Nat. Comm. **13,** 2472 (2022)

$TaSe_2$ monosheet prepared by Ta/Bi_2Se_3(0001) interface reaction

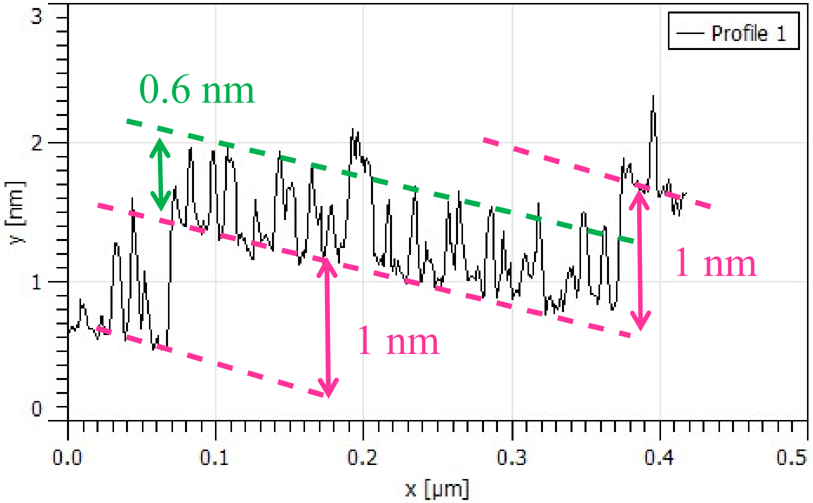

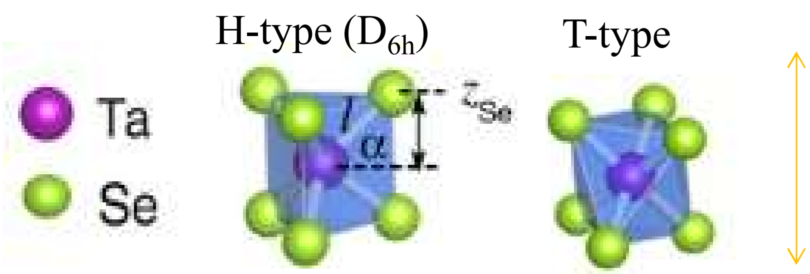

Triple Layer
6.2 Å

Symmetry breaking in the two-dimensional limit: single $TaSe_2$ layer

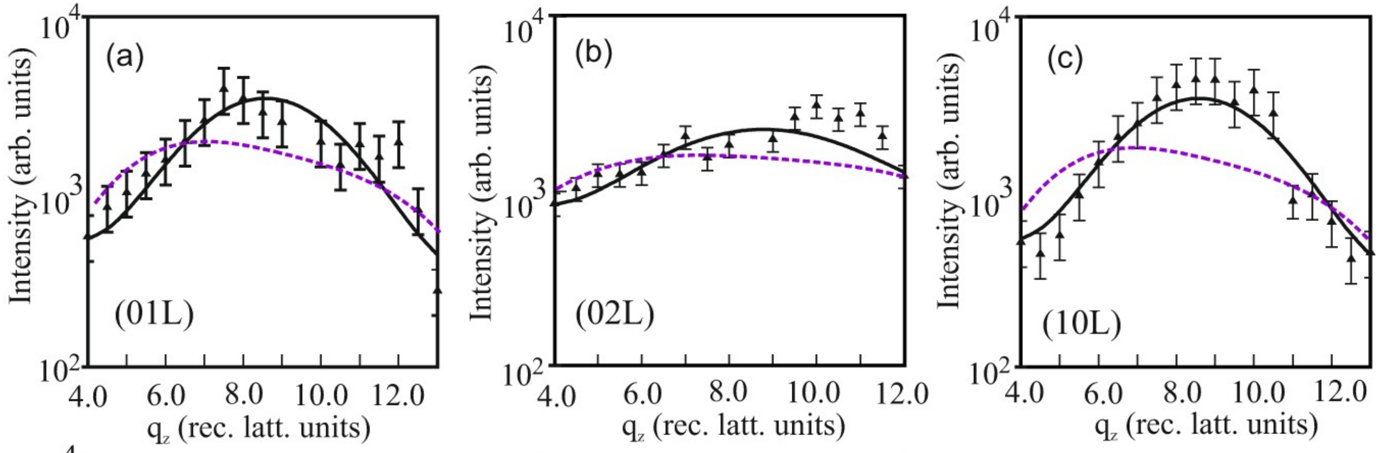

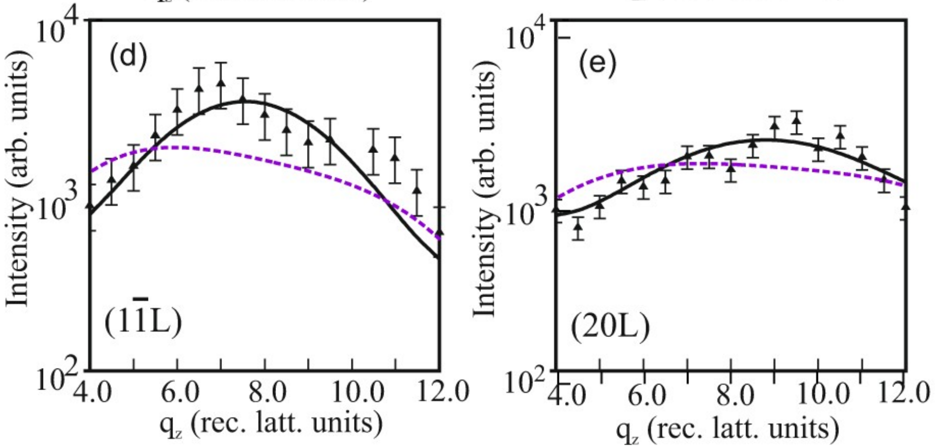

1H

1T

Data and fit:
Rod-like intensity distribution along q_z

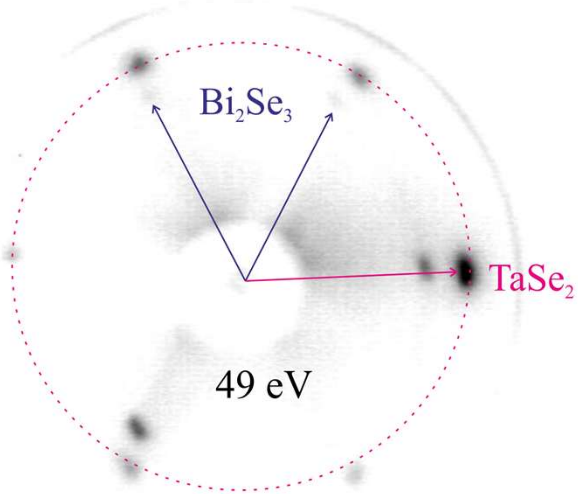

J. Rubio-Zuazo
G. Castro
(BM25b)

Symmetry breaking in the two-dimensional limit: 1H-$TaSe_2$

$TaSe_2$ monosheet: Fermi Surface: Symmetry lowering D_{6h} -> D_{3h} -> C_{3v}: In-plane spin component appears

Electronic structure in unrelaxed monosheet

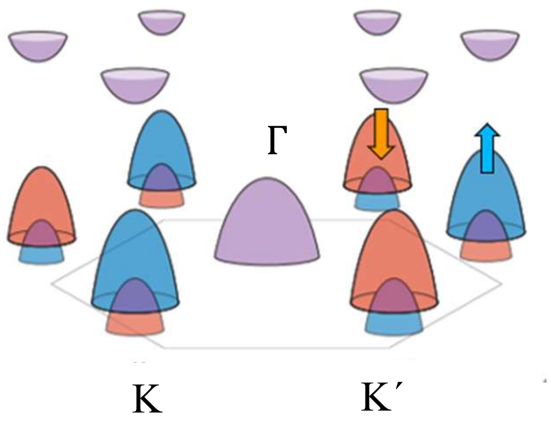

Inversion symmetry in the bulk ($P6_3/mmc$)
In monosheeet: D_{3h} >> degeneracy lifted
+strong SOC > ISING SPINS

A. Polyakov, et al. Nat. Comm. **13,** 2472 (2022)

XRD structure analysis

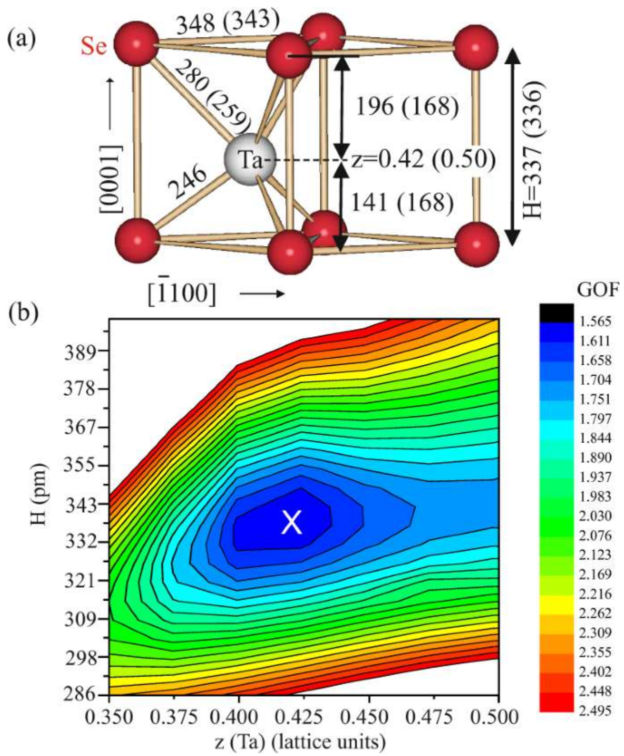

Spin-resolved photoemission (Elettra Synchrotron)

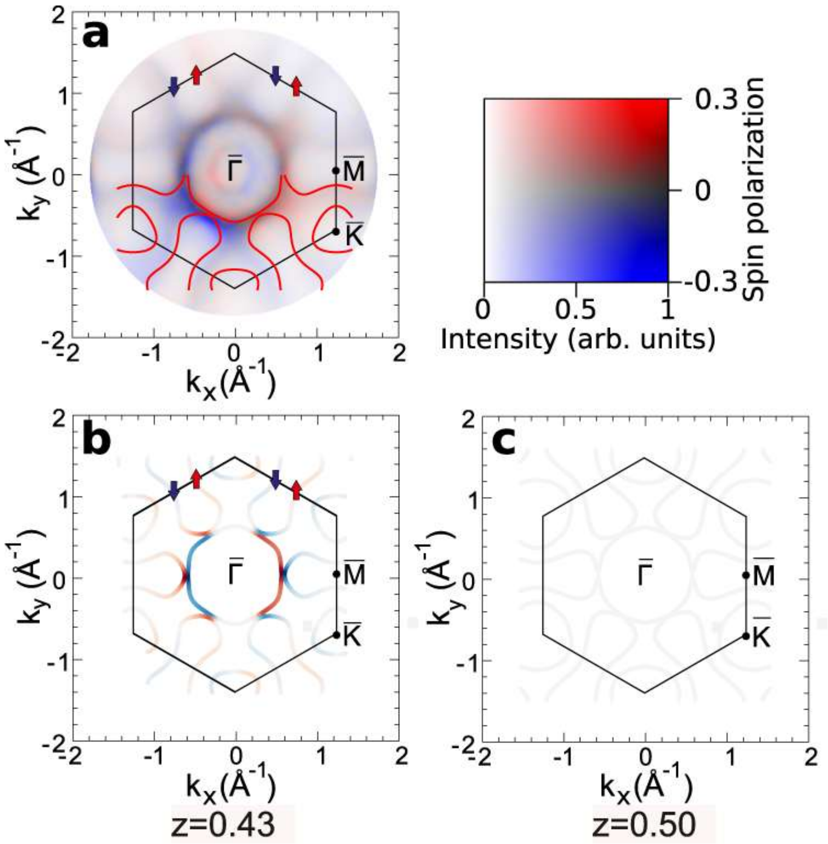

In- house high-brilliance X-ray source: Ga-jet & six-circle diffractometer

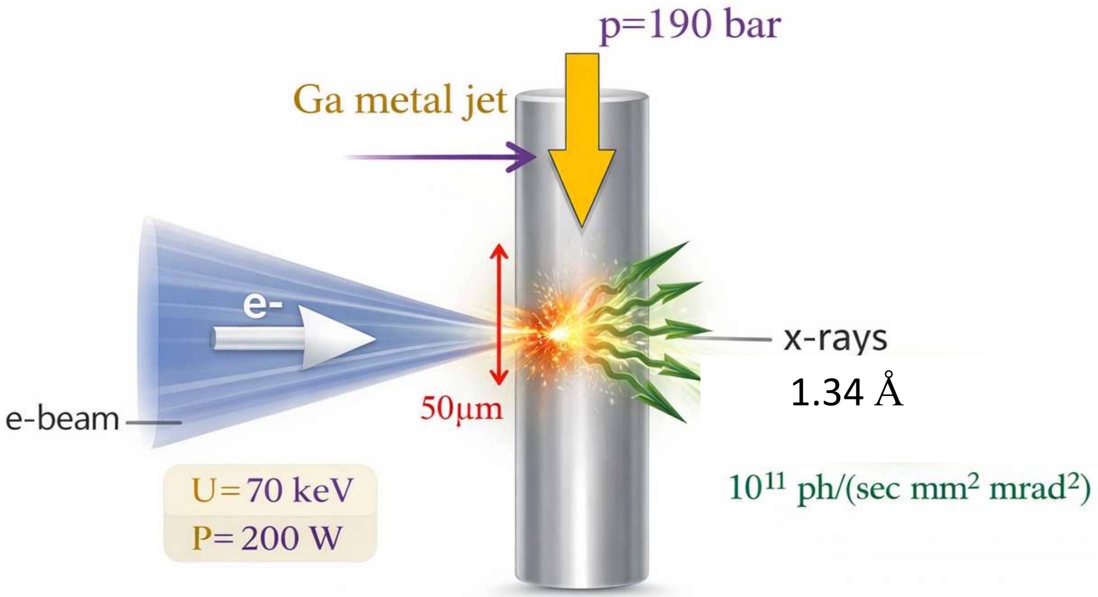

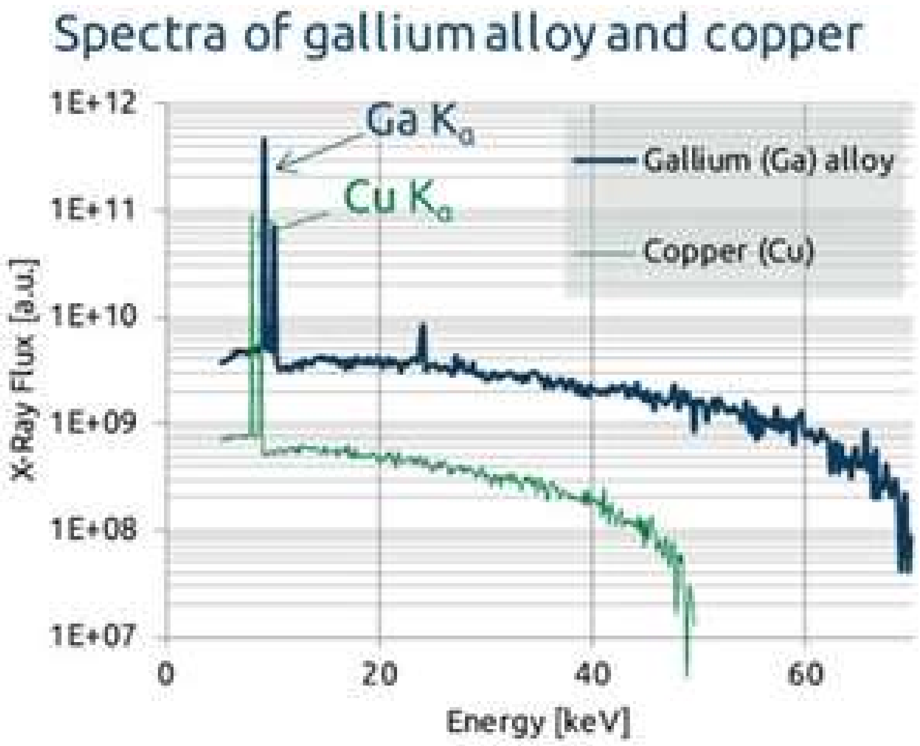

www.excillum.com

In-house X-ray diffraction using GaJet X-ray source

Six-circle diffractometer (z-axis)
Pilatus 2D pixel detector

Ga jet x-ray source & Montel optics

Cryostate (4-500 K)

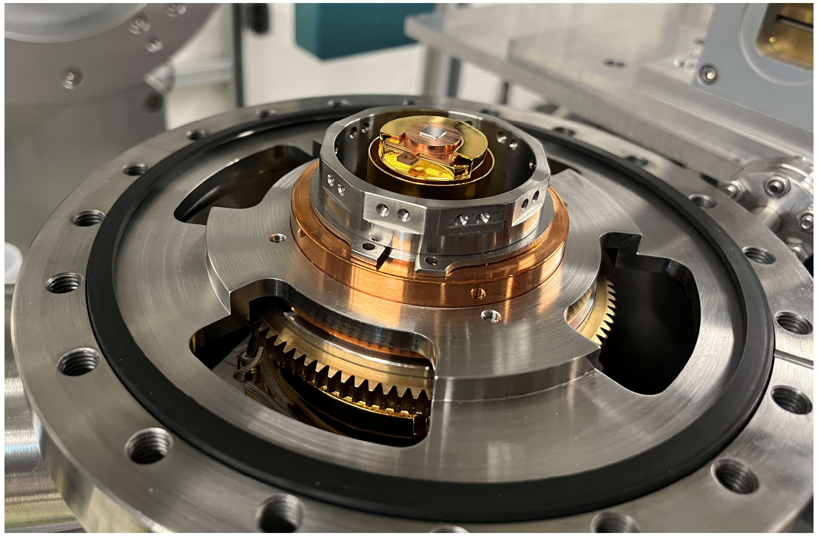

Fe_3GeTe_2 : Van der Waals material w/o inversion symmetry >> Neél Skyrmions

- **Symmetry *P*3*m*1 (#156)**
- **NOT $P6_3/mmc$**

- **Hosts Néel skyrmions**.

XRD
Charge density

vdW gap

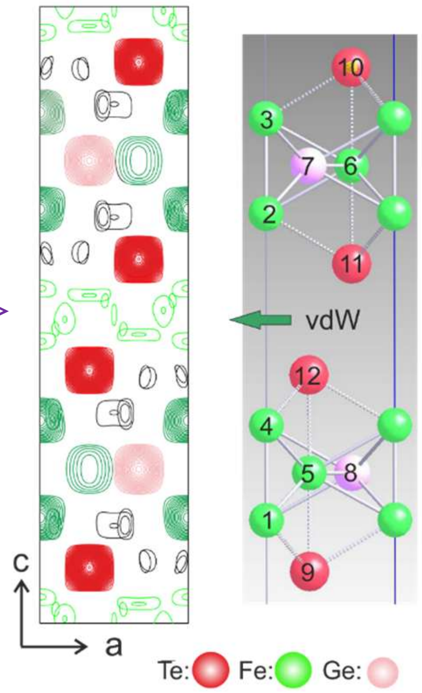

Chakraborty et al., Advanced Materials 2022, **34**, 2108637

Experiment

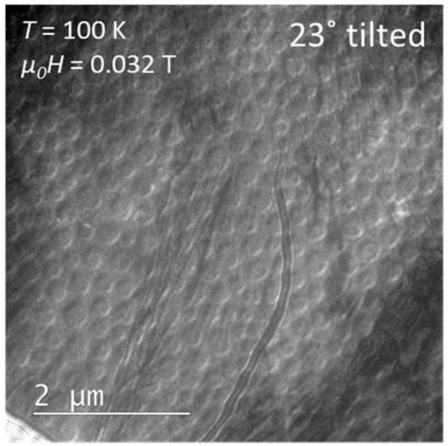

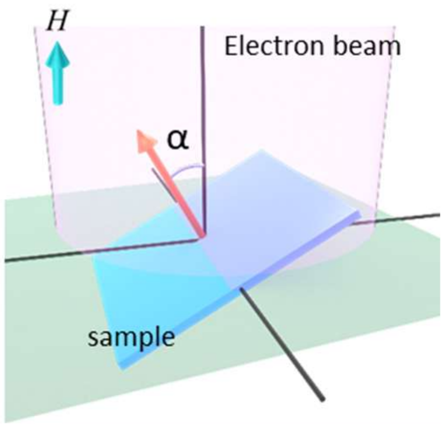

Simulation

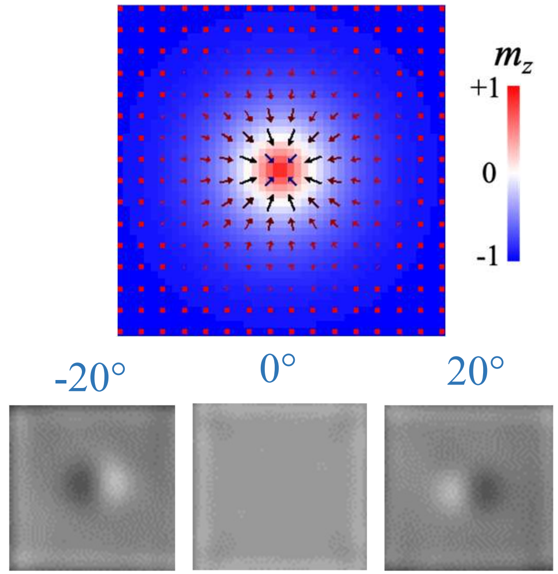

[1] A. K. Srivastava et al., Adv. Mater. 1904327 (2019)
[2] C. Chakraborty et al., Adv. Mater. 2108637 (2022)
[3] R. Saha et al., Nat. Commun. 13, 3965 (2023)
[4] A. Gopi et al., ACS Nano 18, 5335 (2024)
[5] R. Saha et al., npj Spintronics 2, 21 (2024)
[6] M. Silinskas et al., Phys. Rev. Lett. 133, 256702 (2024)

Van der Waals materials: Fe_3GeTe_2

Observation of "forbidden" reflections in SGR $P6_3/mmc$

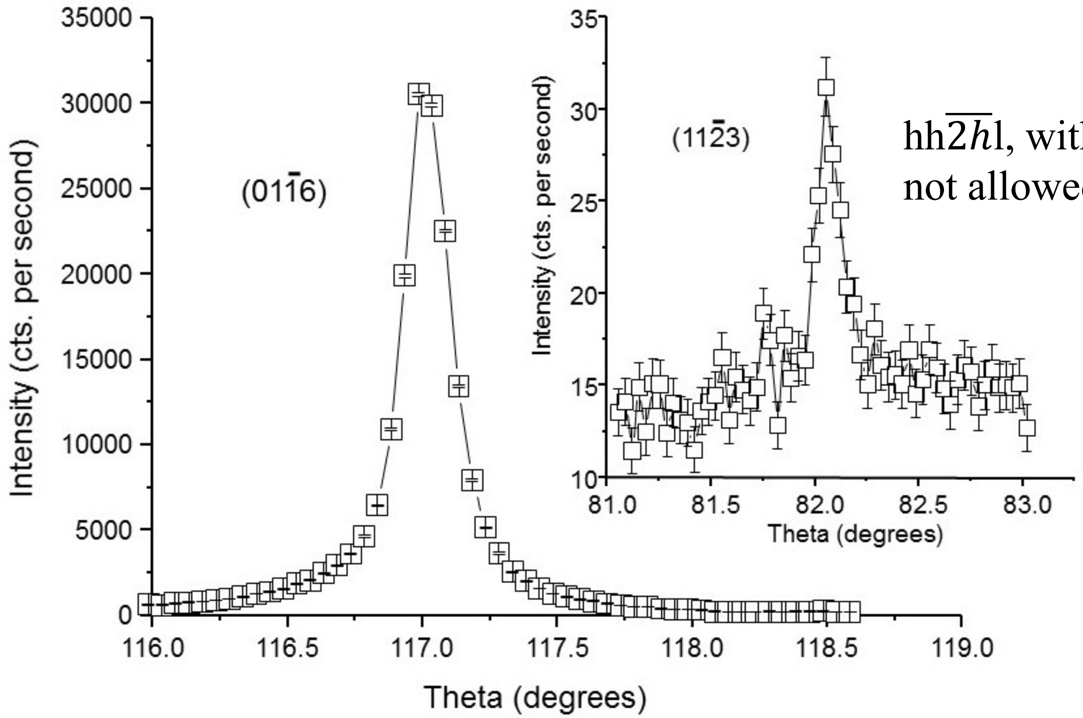

hh$\overline{2h}$l, with l odd
not allowed in $P6_3/mmc$

[1] A. K. Srivastava et al., Adv. Mater. 1904327 (2019)
[2] C. Chakraborty et al., Adv. Mater. 2108637 (2022)
[3] R. Saha et al., Nat. Commun. 13, 3965 (2023)
[4] A. Gopi et al., ACS Nano 18, 5335 (2024)
[5] R. Saha et al., npj Spintronics 2, 21 (2024)
[6] M. Silinskas et al., Phys. Rev. Lett. 133, 256702 (2024)

Van der Waals materials: Fe_3GeTe_2 : Inversion asymmetry >> Neél Skyrmions

- Lacks inversion symmetry due to
  1) **an asymmetric occupation of Fe sites 5 and 6**
  2) due to the statistical occupation of different sites within the vdW's gap by Fe atoms.

- **Symmetry *P*3*m*1 (#156)**
- **NOT $P6_3/mmc$**

- **Hosts Néel skyrmions**.

Charge density contour
From FT of |Fobs|

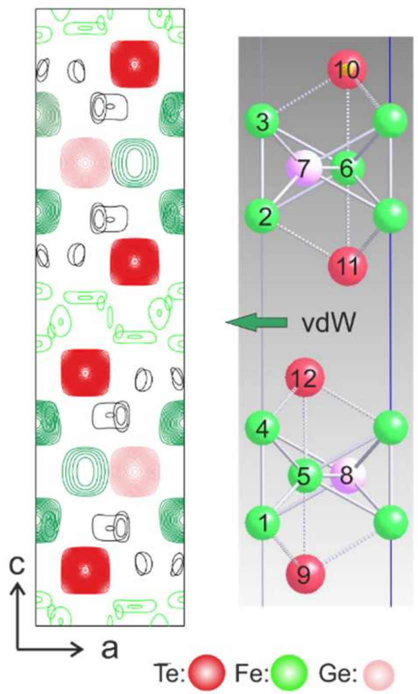

Asymmetric occupancy of Fe sites

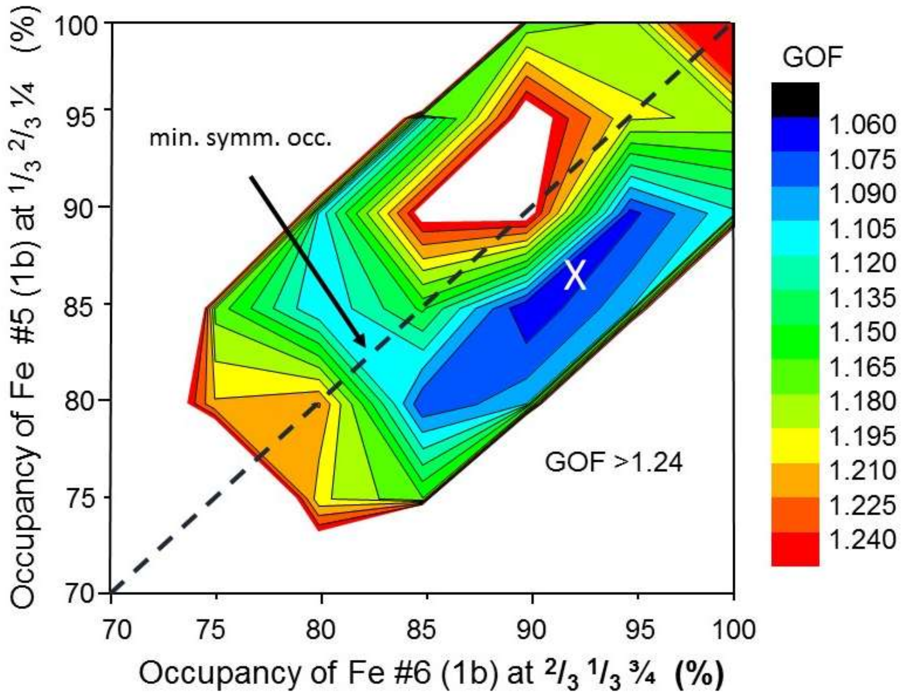

A Chakraborty, et.al.
Adv. Mater. 2022, 34, 2108637

Inversion symmetry breaking by local doping with large ions: Dy in ferrite

Acentric crystal structure -> chirality (DMI)
Many crystal structures are centrosymmetric
How can they be made acentric?

Strain gradient by epitaxy

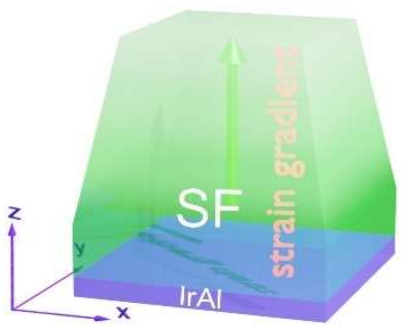

Doping with large atoms

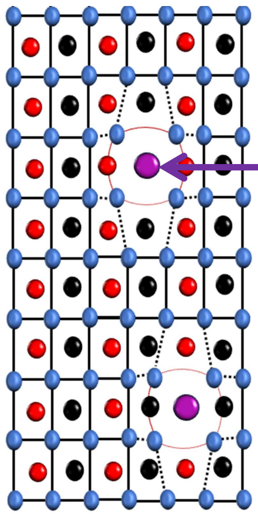

large dopant atom
local strain gradient

$NiFe_2O_4$
collinear ferrimagnet

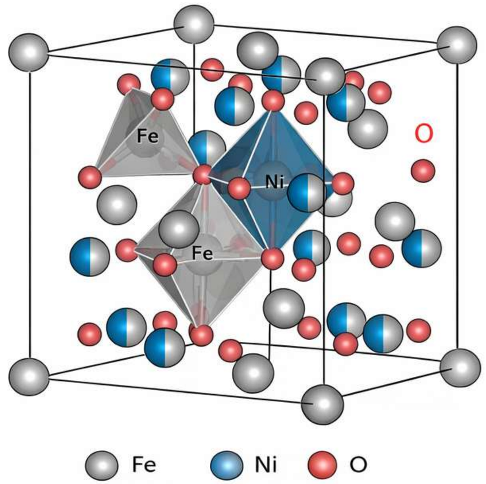

$r_{Dy3+} = 0.91Å$
$r_{Fe3+} = 0.65$ Å
$r_{Ni2+} = 0.69$ Å

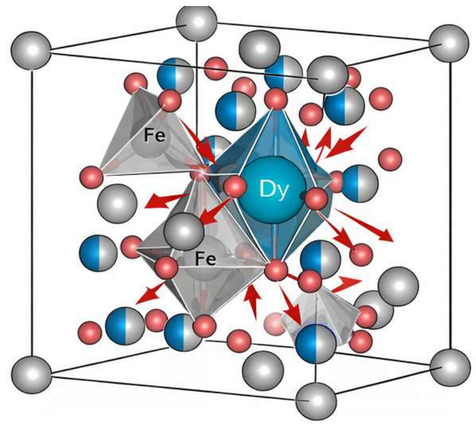

Inversion symmetry breaking by local doping with large ions: XRD

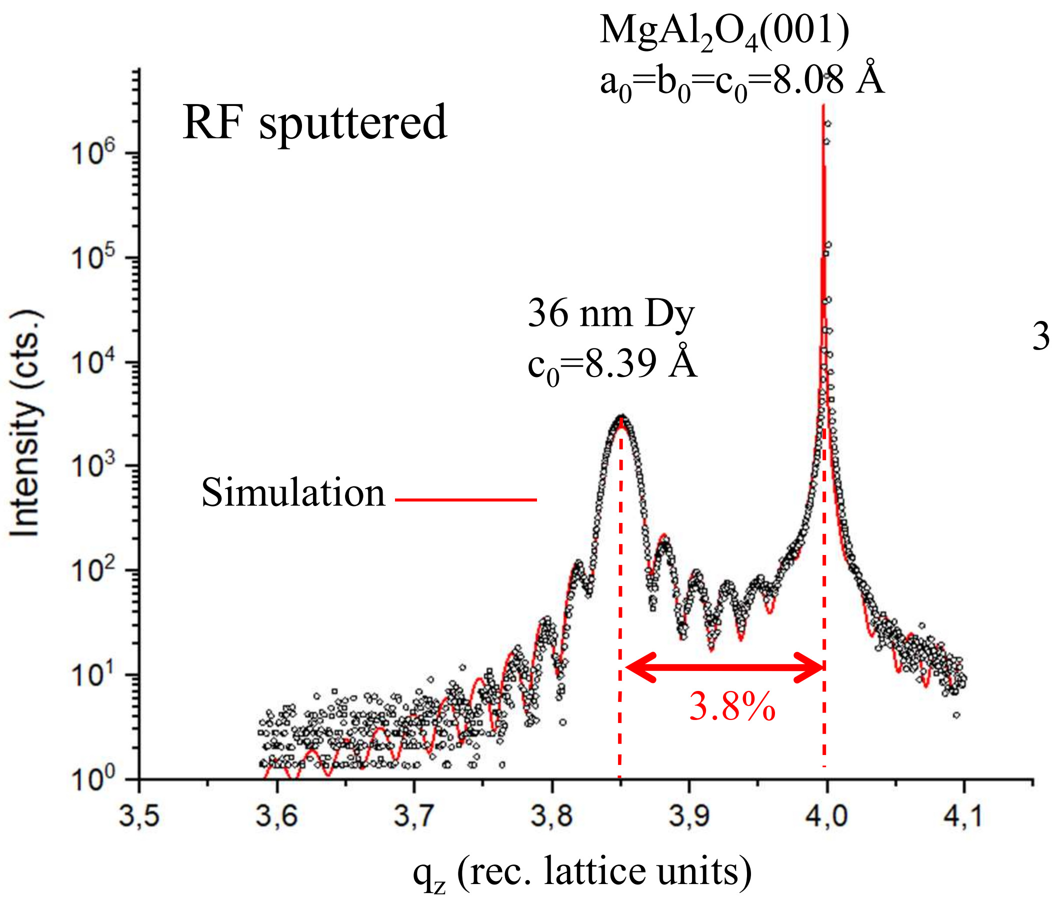

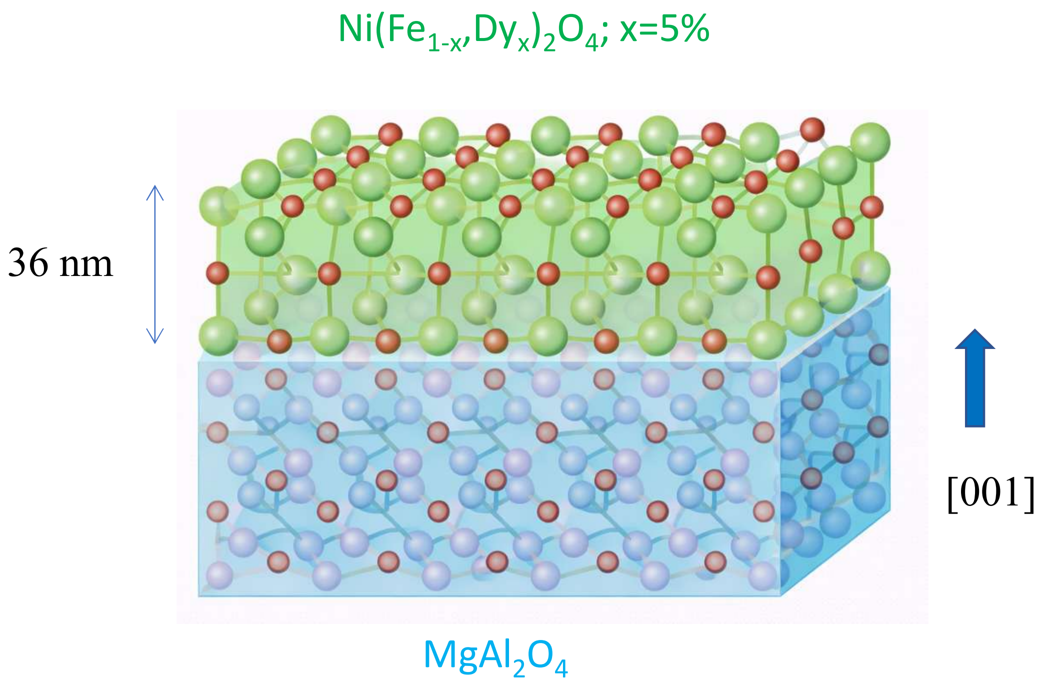

Inversion symmetry breaking by local doping with large ions: EXAFS @ Dy-L_3

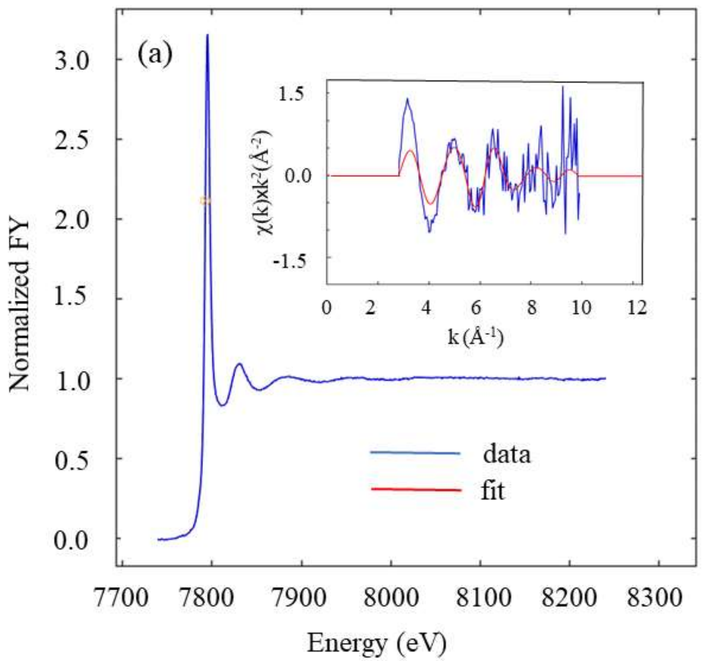

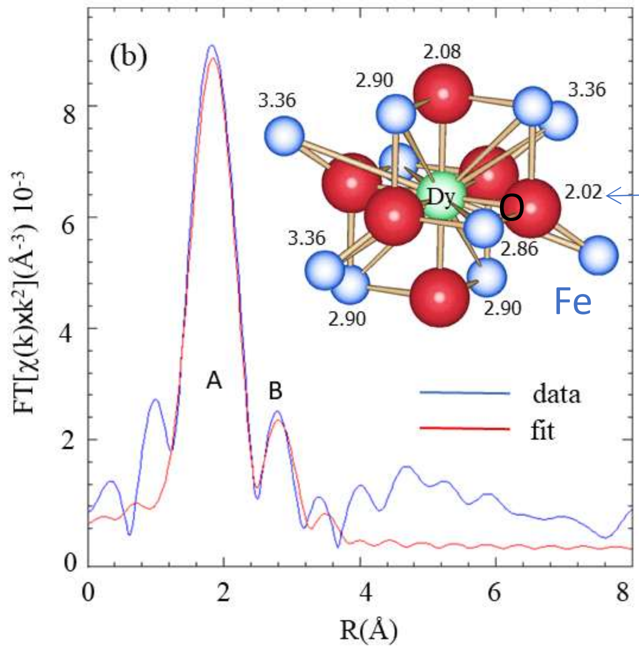

Dy in O_h site:

Distances R_B (Å) calculated for unstrained structure using XRD data:

a=b=8.08 Å
c=8.39 Å

$$\frac{\mu-\mu 0}{\mu 0} \propto \sum_i \frac{S_0^2 \cdot N_i^* \cdot F_i(k)}{k \cdot R_i^2} \cdot \sin[2kR_i + \delta_i(k)]$$

Shell	R_B (Å)	N	R(Å)	N*	σ^2(Å^2)	DE$_0$ (eV)
O	2.02; 2.08	6	2.33(1)	6.0*	0.009	2.5
Fe	2.86; 2.90	6	3.33(3)	4.0*	0.012	-1.6
Fe	3.36	4	3.59(3)	4.0*	0.012	1.9

SOLEIL SYNCHROTRON
E. Fonda

Resonant magnetic scattering of soft x-rays: Second order perturbation

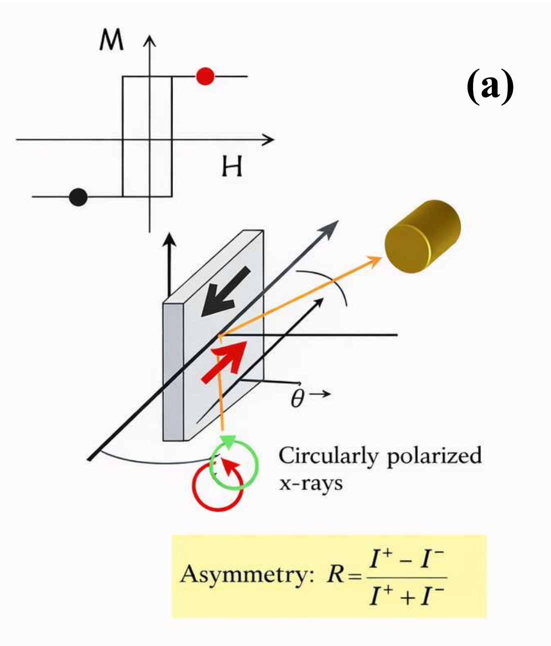

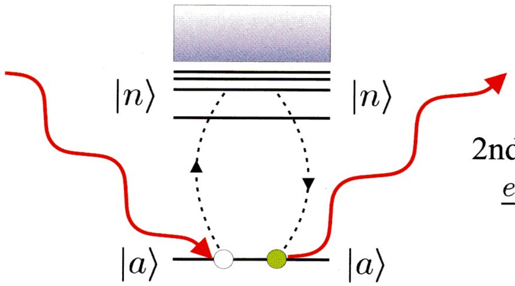

2nd order: $\frac{e\mathbf{A}\cdot\mathbf{p}}{m}$

$Ni^{2+}:O_h$

X-ray absorption at Fe-$L_{2,3}$

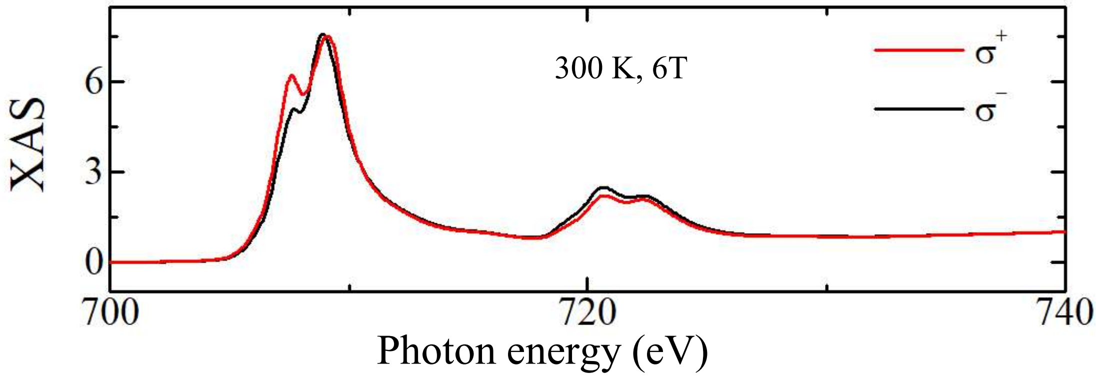

Second order perturbation theory

$$W = \frac{2\pi}{\hbar}\left|\langle f|H_I|i\rangle + \sum_n \frac{\langle f|H_I|n\rangle\langle n|H_I|i\rangle}{\hbar\omega - E_i - E_n}\right|^2 \rho(\varepsilon_f)$$

First observation in Holmium by: D. Gibbs, D.R. Harshman, E.D. Isaacs, D.B. McWhan, D. Mills, and C. Vettier, Phys. Rev. Lett. 61, 1241 (1988)

Soft X-ray resonant magnetic reflectivity. Data and fit: Analysis of spin texture

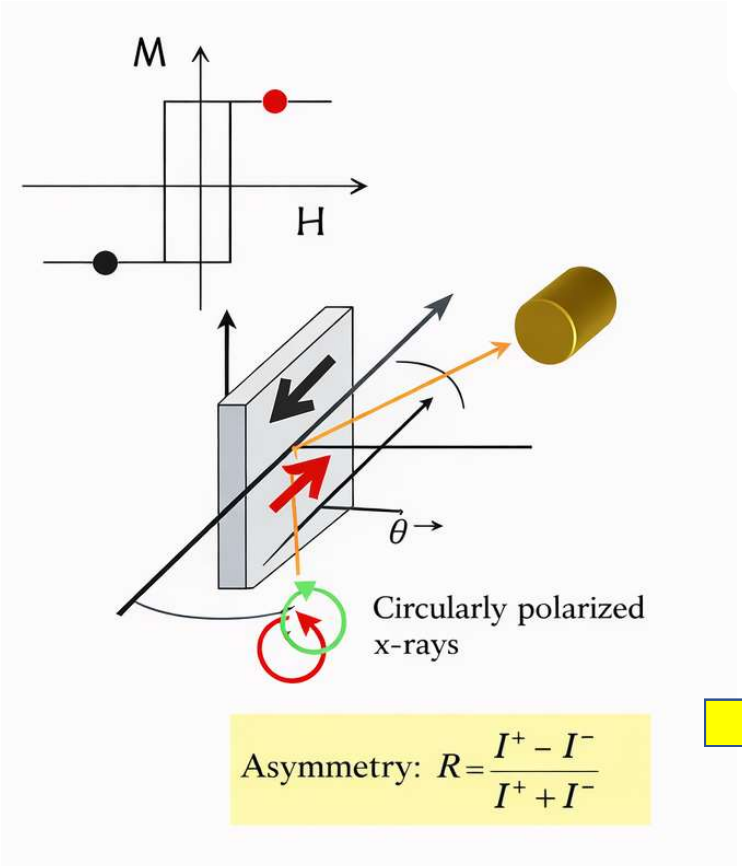

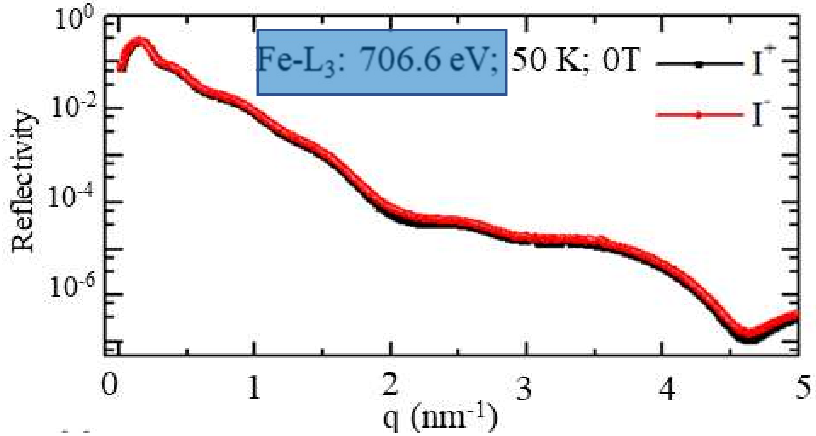

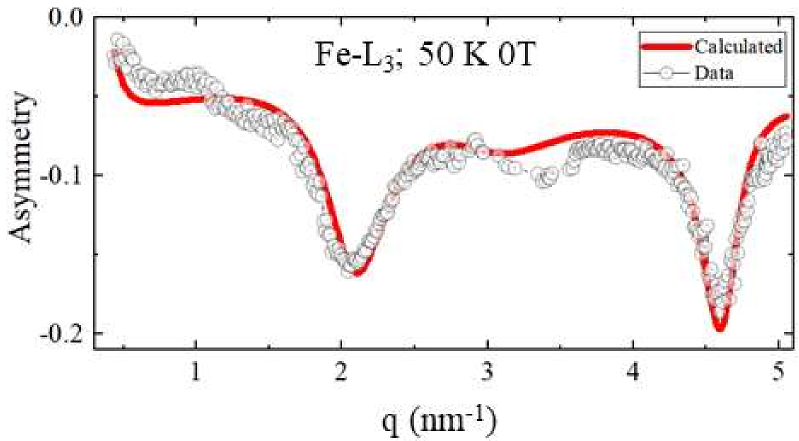

M. Valvidares
P. Gargiani

ALBA

Soft X-ray resonant magnetic reflectivity: Quantitative analysis of spin texture

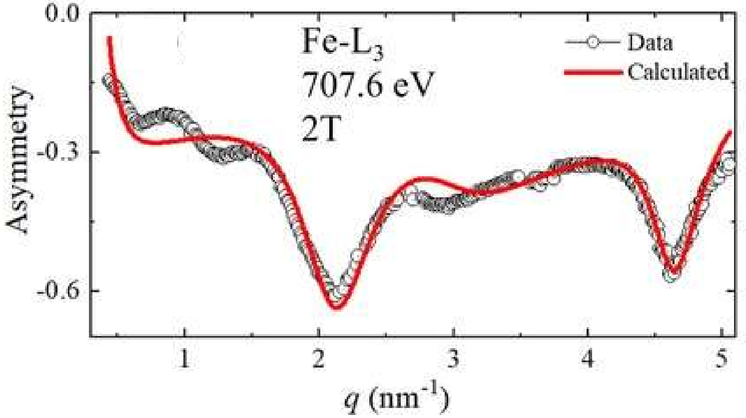

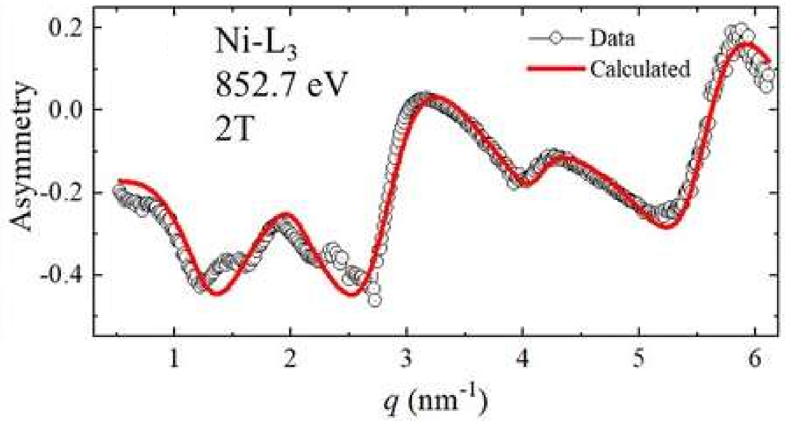

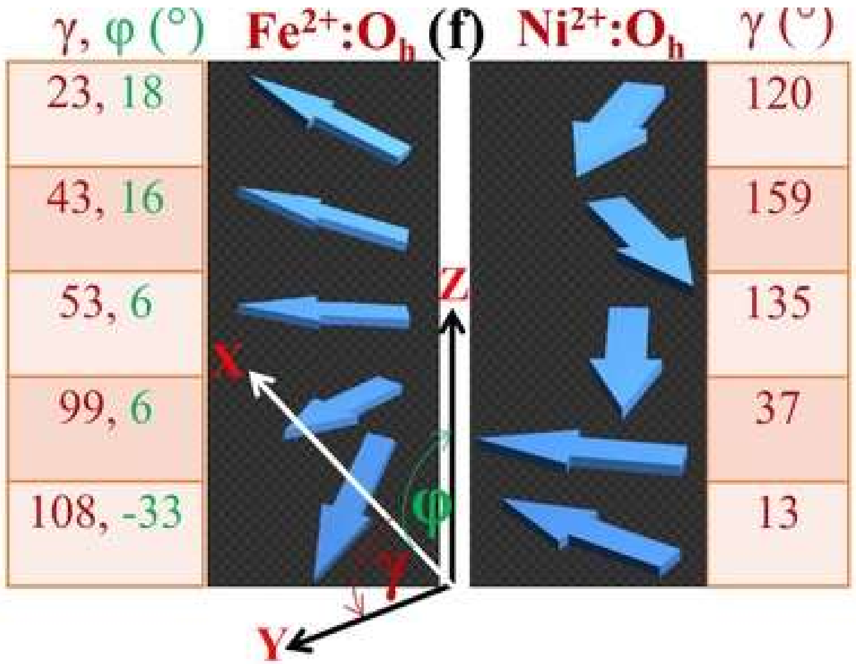

Soft X-ray resonant magnetic reflectivity: Quantitative analysis of spin texture

Magneto-optic approach:
Calculates iteratively reflectivity and transmission at each interface from the bottom to the top

[I.G. Parratt, Phys. Rev. **95**, 359 (1954);
J. H. Underwood & T. W. Barbie, Appl. Optics **20**, 3027 (1981).

I=| R:T |²

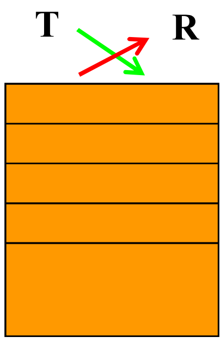

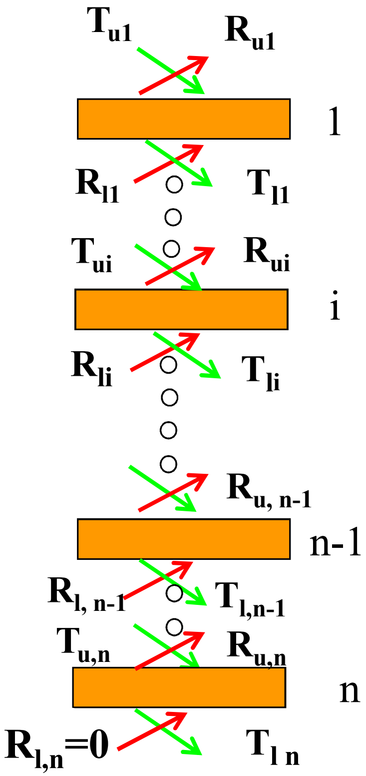

$$n(E)=1-\sum_i N_i r_e \lambda^2 f_i/2\pi = 1-\delta(E)+i\beta(E)=\sqrt{\varepsilon(E)}$$

$$\overline{\overline{\varepsilon}} = \begin{pmatrix} \varepsilon & i\eta\cos\varphi & -i\eta\sin\gamma\sin\varphi \\ -i\eta\cos\varphi & \varepsilon & i\eta\cos\gamma\sin\varphi \\ i\eta\sin\gamma\sin\varphi & -i\eta\cos\gamma\sin\varphi & \varepsilon \end{pmatrix}$$

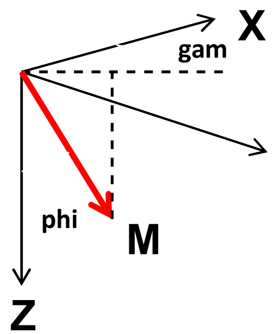

$$\varepsilon = 1-\varepsilon_r - i\ \varepsilon_i = 1-\frac{Nr_0\lambda^2}{\pi}\left(Z+f'(E)+i\ f''(E)\right)$$

$$\eta = 1-\eta_r - i\ \eta_i = 1-\frac{Nr_0\lambda^2}{\pi}\left(m'(E)+i\ m''(E)\right)$$

Thank you for your attention.

http://www.mpi-halle.mpg.de